Somruedee Klaithong, Daniel Van Opdenbosch, Cordt Zollfrank and Johann Plank*

Preparation of magnesium oxide and magnesium silicate replicas retaining the hierarchical structure of pine wood

DOI 10.1515/znb-2016-0241 Received November 23, 2016; accepted December 16, 2016

Abstract: Replicas retaining the structural characteristics of softwood (Pinus sylvestris) were obtained by infiltrating pretreated templates with a methanolic methoxymagnesium methyl carbonate (MeOMgOCO, Me) solution as a precursor which then hydrolyzed into MgCO₃ nanoparticles. Subsequent calcination at temperatures ranging from 500 to 1450°C vielded annealed MgO replicas on levels of hierarchy from the macroscopic to the submicron scale. The mechanical stability of the replicas could be improved through calcination at 1450°C. However, this treatment leads to considerable shrinkage ($\Delta_{ax} = 56\%$). Even more stable MgO replicas were obtained by infiltrating the pine template first with MeOMgOCO, Me, followed by a second infiltration step with an ethanolic tetraethyl orthosilicate (TEOS) solution and subsequent calcination at 1350°C. The resulting replicas constitute an MgO framework overgrown with Mg₂SiO₄ (forsterite) and exhibit compression strengths of 31±8 MPa, as well as hierarchical structures combined with an anisotropic porosity.

Keywords: biotemplating; hierarchical structure; magnesium oxide; magnesium silicate; wood template.

1 Introduction

Silica aerogels are highly attractive materials because of their exceptional thermal insulating property resulting from the Knudsen effect [1]. They can be fabricated, e.g. via a sol-gel process utilizing an alkoxysilane as

*Corresponding author: Johann Plank, Lehrstuhl für Bauchemie, Technische Universität München, Lichtenbergstraße 4, 85747

Garching, Germany, Fax: +49-89-289-13152, E-mail: sekretariat@bauchemie.ch.tum.de

Somruedee Klaithong: Lehrstuhl für Bauchemie, Technische Universität München, Lichtenbergstraße 4, 85747 Garching, Germany

Daniel Van Opdenbosch and Cordt Zollfrank: Chair für Biogenic Polymers, Technische Universität München, Schulgasse 16, 94315 Straubing, Germany precursor [2, 3]. Aerogels possess a non-hierarchical porosity across the matrix which in some applications is undesirable. However, for certain purposes a three-dimensional hierarchy associated with anisotropic porosity is advantageous. For example, hierarchical structures provide higher chances to trap particles with different diameters in fibrous membranes applied for air filtration [4]. Another example where hierarchically porous morphologies are desirable are, e.g. lithium-ion batteries. A nanoporous structure accelerates lithium ion intercalation/deintercalation and electron transport, and enlarges the electrode–electrolyte interphase area, while micronsized assemblies provide high volumetric density, easy processability and electrode integrity [5].

Wood has been identified as a versatile template exhibiting a hierarchical structure [6]. Spruce wood is a soft-wood consisting of parallel tube-like wood cells, the tracheid fibers, with diameters in the range of $10-40~\mu m$. In the cell walls of the tracheid fibers, cellulose fibrils are accompanied by polyoses which are embedded altogether in a lignin matrix [7]. The cellulose elementary fibrils are partly crystalline and exhibit a thickness of around 2.5 nm. The fibrils spiral the lumen at the characteristic microfibril angle [8].

The advantage of using wood as a template is an easy access to hierarchically porous materials [6]. To achieve a good replication, the wood template needs to be extracted with organic solvents in order to remove inorganic impurities, followed by partial delignification with sodium chlorite to open up the pore structure for accessibility of the precursor molecules [9, 10]. In this manner, a successful nanoscopic replication of cellulose fibrils was fabricated by infiltrating tetraethyl orthosilicate (TEOS) into delignified spruce wood followed by calcination [11]. During the calcination step, polyoses decompose between 250 and 300°C, resulting in a silica network in the form of long fibrils exhibiting a diameter of about 10 nm, embedded in the partly intact cellulose microfibrils. The cellulose elementary fibrils are further degraded between 350 and 450°C. In their place, corresponding nanopores with diameters of 2 nm are formed. These pores are stable up to 625°C, beyond which sintering occurs [12]. Furthermore, other groups have prepared tailor-made precursor sols

and salt solutions and used them to fabricate hierarchically Eu-doped Y₂O₃ from softwood [13–15].

Owing to their nanoporosity, calcium carbonate aerogels have recently been proposed as potential replacements for polystyrene foams contained in heat insulating renders and panels used by the construction industry [16, 17]. Also, magnesium carbonate xerogels and aerogels which consist of networks of magnesium carbonate nanoparticles were produced by controlled hydrolysis of methoxymagnesium methyl carbonate, Mg(OCOOCH₂) (OCH_a) (MeOMgOCO_aMe) [18]. These aerogels composed of alkaline earth metal compounds are of special interest for construction applications because of their high compatibility and inertness towards cement [18]. Furthermore, such porous materials are also interesting as functionalized supports for other applications, for example the adsorption of heavy-metal ions from aqueous solution using mercapto-modified silica particles [19].

Magnesium silicate (forsterite), Mg₂SiO₄, constitutes the most abundant mineral in the Earth's upper mantle and transition zone [20]. Because of the exceptionally high fracture toughness of forsterite, this material has been proposed as a potential alternative to calcium phosphate bioceramics [21]. Through calcination of the wet gel obtained from Mg(NO₂)₂ · 6H₂O and colloidal SiO₂ in a sol-gel process at 1450°C, forsterite ceramics with exceptionally high bending strength and fracture toughness, even superior to those of currently known hydroxyapatite ceramics, were obtained [22]. Furthermore, forsterite nanopowder was produced via a sol-gel process [23, 24]. In a study of the sinterability of forsterite powder synthesized via solid-state reaction using MgO and talc (Mg₂Si₄O₁₀(OH)₂) it was found that the mechanical properties were improved when the calcination temperature was increased from 1200 to 1400°C. However, higher sintering temperatures led to grains larger than ~22 µm, resulting in lower values of hardness and fracture toughness [25]. The product formed was phase-pure forsterite, and no decomposition into phases such as MgO or enstatite was observed. Furthermore, nanostructured forsterite bioceramics were shown to possess excellent mechanical properties and thus can be used as a bioactive bone tissue engineering material [24].

In previous research, we have synthesized a CaCO replica of hierarchically structured spruce wood by infiltrating pretreated wood specimens with a solution of calcium di(methylcarbonate) in methanol. This precursor hydrolyses into a CaCO₂ sol [26, 27]. However, the disadvantage of these CaCO3 replicas is their poor mechanical stability which limits their use, e.g. for construction applications. In the present work we investigate the fabrication

of hierarchically structured MgO replicas. It was hoped that the MgO replicas would exhibit higher mechanical stability than the previously synthesized porous MgCO₂ monoliths [18] by using MeOMgOCO, Me as a magnesium precursor and subsequent hydrolysis into a MgCO, sol inside the wood cell walls. After infiltration, the cellulose matrix was removed by calcination at temperatures ranging from 500 to 1450°C yielding porous monoliths composed of MgO nanoparticles. The calcination temperature was varied in order to study its effect on the MgO particle size, the quality of replication and the mechanical stability of the replicas. Additionally, magnesium silicate replicas exhibiting high compressive strength were synthesized by infiltrating the MgO replica with an alkoxysilane precursor and subsequent calcination at 1350°C. For this system, the temperature-dependent formation of different magnesium silicates was studied.

2 Results and discussion

2.1 Magnesium carbonate precursor

The concept of wood replication with MgO was based on the hydrolysis of methoxymagnesium methylcarbonate as a precursor, as was reported earlier [18]. For this purpose, magnesium methanolate was prepared by reacting magnesium metal with methanol (eq. 1) [28, 29]. Subsequent bubbling of gaseous CO, through this solution results in methoxymagnesium methylcarbonate which physically binds an additional amount of CO₂ (eq. 2) [18, 30]. The structure of this compound has been confirmed in an earlier work [18]. Using IR and elemental analysis it has been shown that CO, inserts into one methylate group resulting in Mg(OCO₃Me)(OMe). The clear solution (solid content 4.9 mass%) thus obtained was used in the following infiltration process. Dynamic light scattering showed that no sol particles were present in the MeOMgOCO, Me solution prior to infiltration. It revealed that sol particles in the range of 0.6 to 11.0 nm were formed only after additional water was added to the MeOMgOCO, Me solution. However, such sol particles would be unable to diffuse into polyoses [12, 27]. Therefore, it can be hypothesized that the MeOMgOCO Me solution reacts with the moisture inside the wood cell wall to form a sol and, most likely, later a gel. Consequently, MgCO3 was obtained from the magnesium precursor (eq. 3). After calcination in air, the macroscopic and submicron scale structure of the wood was replicated. However, depending on the number of infiltration steps and the calcination conditions, materials with different structures were obtained, as discussed in the following.

The infiltration process was assessed by elemental mapping of magnesium in a cross section of the sample embedded in paraffin, performed after one infiltration. It revealed that magnesium was present only in the wood cell walls, indicating that the magnesium precursor had penetrated them and therein had formed hydrated MgCO. (nesquehonite) [X-ray diffraction (XRD) not shown here] (Fig. 1). The voids between the cell walls originated from the delignification process.

$$Mg + 2 CH_3OH \rightarrow Mg(OCH_3)_2 + H_2 \uparrow$$
 (1)

$$Mg(OCH_3)_2 + (1+x)CO_2 \rightarrow Mg(OCOOCH_3)(OCH_3) \cdot xCO_2$$
 (2)

$$Mg(OCOOCH3)(OCH3) \cdot xCO2 + H2O \rightarrow MgCO3 + 2 CH3OH + xCO2 \(\backsquare{1}\) (3)$$

2.2 Preparation of MgO replicas

A replica of the delignified pine wood sample was produced by infiltrating the pretreated template one time with MeOMgOCO₂Me solution, followed by calcination at 500°C for 2 h to completely remove all organic matter. The resulting product constituted a positive, yet very fragile MgO replica of the original wood template, whereby the hierarchical structure was reproduced by annealed submicron-sized MgO particles possessing diameters of 200-500 nm (Fig. 2a). As a result of this particulate structure, the MgO replica presented a fragile body exhibiting poor mechanical stability and high shrinkage ($\Delta_{rad} = 26\%$ and Δ_{tan} = 25%; determination of Δ_{ax} was not feasible). XRD analysis revealed that the sample consisted of the polymorph periclase of MgO (Fig. 3a).

2.3 Effect of multiple infiltration

In order to improve the mechanical stability of the replica, three parameters were considered: The amount of precursor infiltrated, the calcination temperature and additional infiltration with an alkoxysilane precursor. At first, repeated infiltration steps were performed with the aim to obtain a more dense assembly of the MgO submicron particles. Such samples were prepared by immersing the pine template twice in the Mg precursor solution and subsequent calcination at 500°C for 2 h. After the first infiltration, the samples were kept at 80°C for 5 h before the second immersion step was conducted and calcination was performed. The resulting product was still fragile, but its mechanical stability had improved noticeably compared to the sample obtained after one infiltration only, providing a compressive strength of 1.0 ± 0.2 MPa (Fig. 4a). This effect can be attributed to the formation of larger and more densely arranged submicron MgO particles (d = 200-600 nm), as observed by scanning electron microscopy (SEM) and lower shrinkage ($\Delta_{rad} = 18\%$ and $\Delta_{tan} = 17\%$; determination of Δ_{ax} was not possible).

Interestingly, the stress-strain curves does not show a linear increase due to elastic deformation, followed by a sharp drop in stress due to final catastrophic failure, as expected in a ceramic material. Instead, the curve shows a linear increase whose inclination drops close to the maximum compressive strength. The material failure is

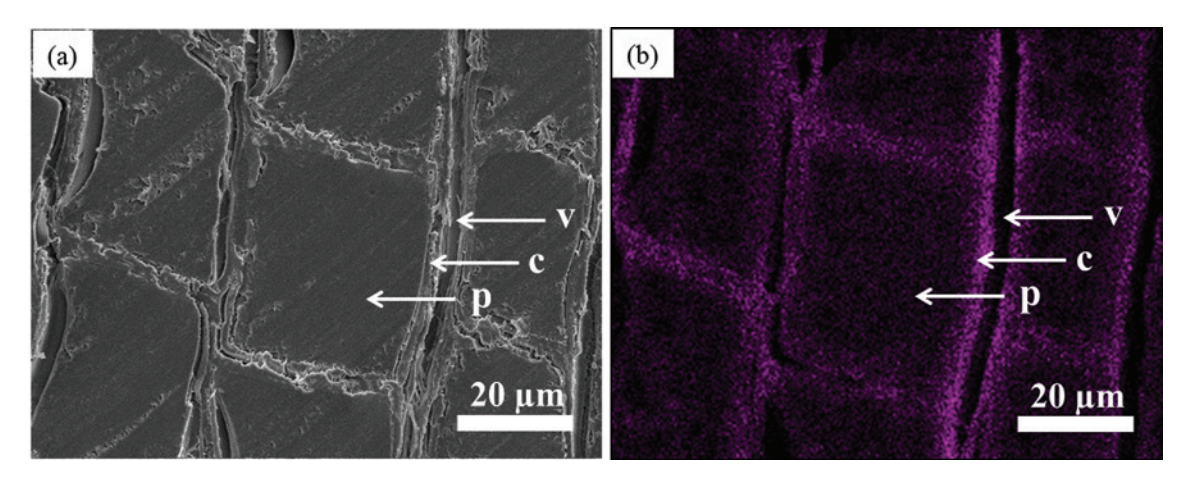


Fig. 1: (a) SEM image of a cross section of a pine wood sample embedded in paraffin after one infiltration with the methanolic magnesium precursor solution (p = paraffin, c = wood cell walls, v = void between wood cell walls), and (b) elemental mapping showing the accumulation of magnesium in the wood cell walls.

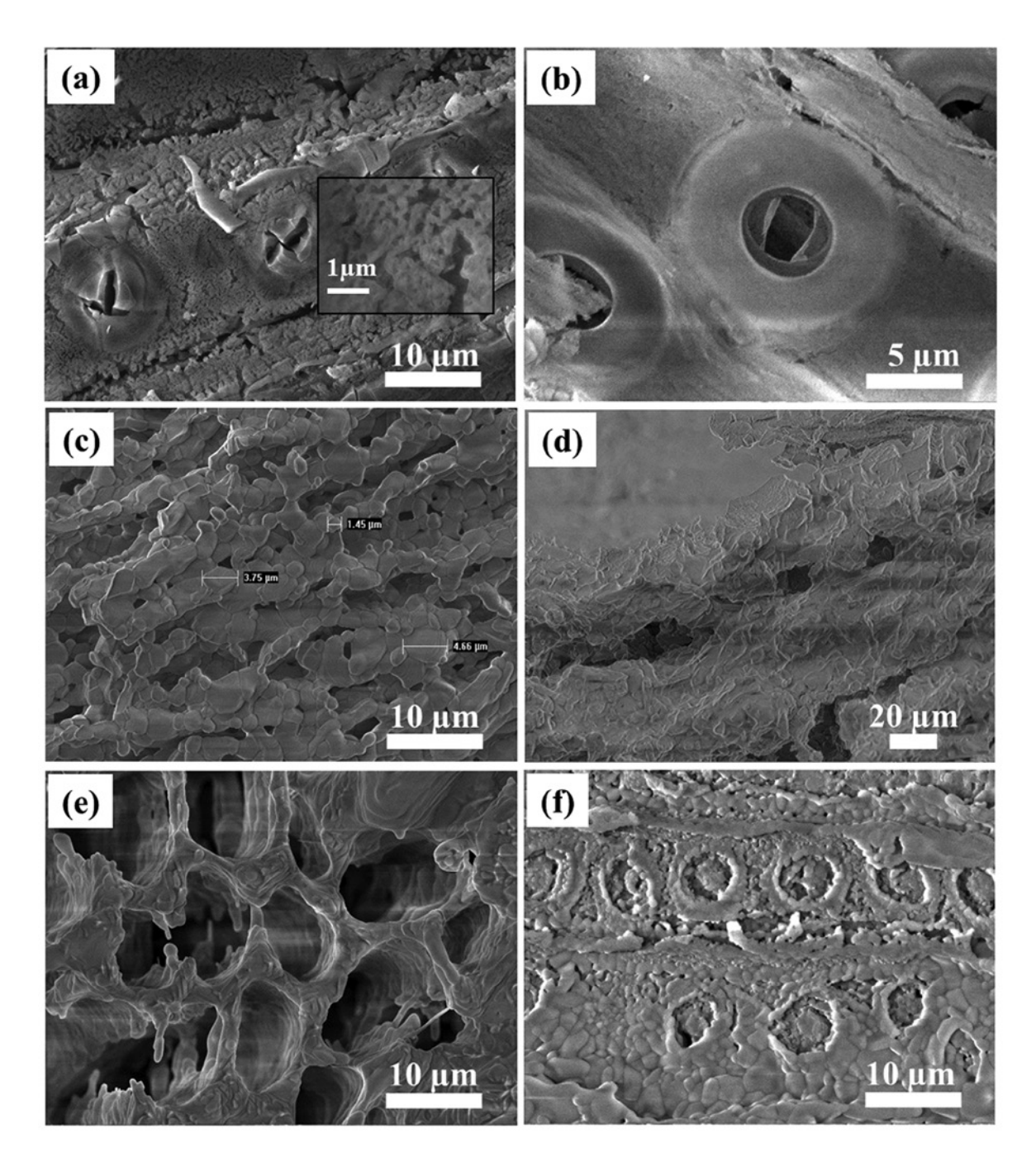


Fig. 2: SEM images of the MgO replicated wood samples: (a) one infiltration with 4.9 mass% MeOMgOCO, Me solution and calcination at 500°C for 2 h; (b) two infiltrations with 0.9 mass% MeOMgOCO_Me solution and calcination at 500°C for 2 h; (c) two infiltrations with 0.9 mass% MeOMgOCO, Me solution and calcination at 1450°C for 5 h; (d) and (e) forsterite/enstatite-replicated wood sample obtained after five infiltrations with 0.9 mass% MeOMgOCO₂Me solution, subsequent soaking with TEOS and calcination at 1350°C for 5 h; and (f) forsterite/ MgO replica from one infiltration with 4.9 mass% MeOMgOCO, Me solution, subsequent soaking with TEOS and calcination at 1350°C for 5 h.

defined by a gradual drop in recorded stress over a compression strain range of more than 20%. We interpret this as a successive fracture of connecting struts or sintering necks, leading to a gradual compaction of the material. We observed that after a compression strain of 30%, the recorded stresses again increased, due to the powdered

sample being compacted. This shows that the retention of the hierarchical wood structure increases the resilience of the material to catastrophic fracture, and allows for a large degree of plastic deformation.

Additional tests involving multiple infiltration steps and calcination at 500°C did not lead to samples

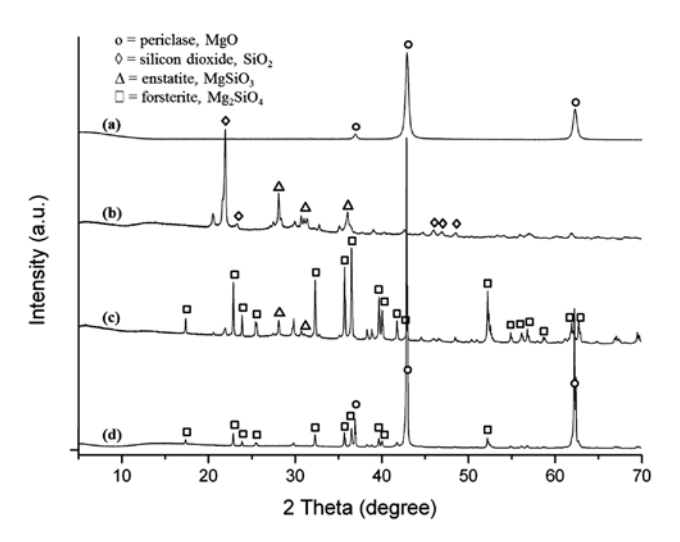


Fig. 3: XRD patterns of the MgO and forsterite replicated wood samples: (a) after thermal treatment at 500°C for 2 h (periclase, MgO: JCPDS 45-0946); (b) after one infiltration with 0.9 mass% MeOMgOCO₂Me solution, subsequent soaking with TEOS and calcination at 1350°C for 5 h (silicon dioxide, SiO₂: JCPDS 14-0260 and enstatite, MgSiO₃: JCPDS 07-0216); (c) forsterite/enstatite obtained from five infiltrations with 0.9 mass% MeOMgOCO₂Me solution, subsequent soaking with TEOS and calcination at 1350°C for 5 h (forsterite, Mg₂SiO₄: JCPDS 89-5130); and (d) formation of forsterite, Mg₂SiO₄ and periclase, MgO after one infiltration with 4.9 mass% MeOMgOCO₂Me solution, subsequent soaking with TEOS and calcination at 1350°C for 5 h.

possessing further enhanced mechanical stability. Thus it was concluded that two infiltration steps represented the optimum with respect to the compressive strength of the sample.

2.4 Effect of low precursor concentration

The most likely infiltration mechanism starts with the methyl carbonate precursors entering the lumen via convection, followed by diffusion into the cell walls driven by concentration gradients [27]. After the infiltration, the liquid phase was evaporated, leading to further condensation of the precursor by loss of alcohol. Since the cell walls provide limited space, a large fraction of the high solid content of the MeOMgOCO₂Me is deposited in the cell lumen, as observed via SEM (Fig. 2a).

In the literature, to achieve SiO₂ replicas that are accurate on the nanometer scale, repeated infiltration with low concentration precursors was found to be suitable [11]. Correspondingly, the solid content of the MeOMgOCO₂Me precursor solution was reduced from 4.9 to 0.9 mass%. Again, calcination was performed at 500°C over 2 h. This

approach led to a more precise replica (the characteristic pit hole structure was better replicated) composed of annealed submicron MgO particles exhibiting diameters of 200–500 nm. Furthermore, the template was infiltrated twice to achieve the desired higher mechanical stability, as presented before. The replica now precisely revealed the characteristic pit holes structure of wood (Fig. 2b). The downside was an even increased shrinkage of $\Delta_{\rm rad}$ = 37% and $\Delta_{\rm tan}$ = 33%.

2.5 Effect of calcination temperature

The samples infiltrated twice with a precursor solution of low solid content (0.9 mass%) were calcined for 5 h at considerably higher temperatures as before, namely at 1000 and 1450°C, respectively. The product obtained at 1000°C was as fragile as the sample calcined at 500°C. However, calcination at 1450°C led to a replica now consisting of larger annealed MgO particles (periclase polymorph, as determined by XRD) with sizes ranging from 600 nm to 5 μm (Fig. 2c). At this temperature, highly annealed MgO particles exhibiting improved mechanical stability compared to the sample calcined at 500°C are formed owed to high particle compaction. Consequently, at this calcination temperature, shrinkage values of $\Delta_{ax} = 56\%$, $\Delta_{rad} = 65\%$ and Δ_{tan} = 62% had occurred. In addition, this product had lost the characteristic microstructure of wood. For example, the pit holes were no longer clearly visible (Fig. 2c).

2.6 Combined treatment with Mg and Si precursors

In another series of experiments, the wood templates were infiltrated once with the magnesium precursor and then additionally immersed in an ethanolic TEOS solution. Alternatively, the imbibition with TEOS was also carried out after calcination of the magnesium infiltrated samples. The consideration behind this consecutive treatment was to coat the initially formed MgO replica with a layer of SiO₂ or magnesium silicate which was expected to further improve the compressive strength of the replica. Calcination was carried out at 1350°C for 5 h. According to literature, this condition produces single-phase forsterite [25, 31]. The sample resulting from one Mg infiltration and TEOS treatment before calcination constituted a monolithic piece containing annealed particles in the range of 500 nm to 3 µm, but it did not show the characteristic structures of wood (pit holes, etc.). XRD patterns revealed that this material consisted of a mixture of silicon dioxide,

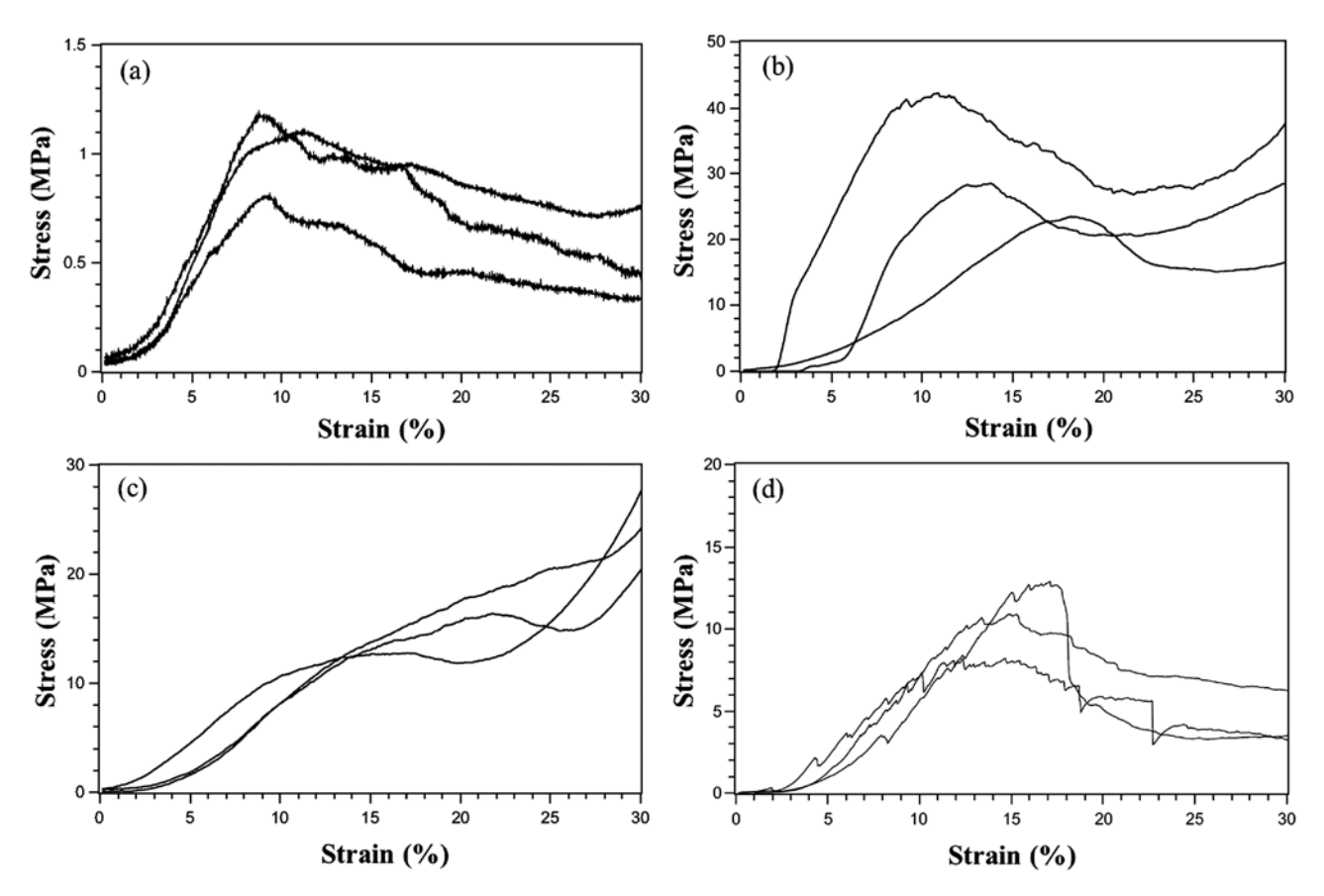


Fig. 4: Compression stress/strain curves of MgO, forsterite and silica replicated wood samples: (a) after 2 infiltrations with 4.9 mass% MeOMgOCO₂Me solution, subsequent calcination at 500°C 2 h; (b) after 5 infiltrations with 0.9 mass% MeOMgOCO₂Me solution, subsequent immersion in TEOS solution and calcination at 1350°C 5 h; (c) after 1 infiltration with 4.9 mass% MeOMgOCO₂Me solution, subsequent immersion in TEOS solution and calcination at 1350°C 5 h; and (d) silica replica prepared after [11]. The three curves shown for each sample represent three independent measurements.

 ${\rm SiO}_2$ and enstatite, MgSiO₃, a metastable phase (Fig. 3b). Apparently, under those conditions there is not enough magnesium precursor present to form the thermodynamically stable forsterite, Mg₂SiO₄.

2.7 Preparation of forsterite replica

In order to increase the amount of magnesium in the sample that is subsequently treated with the alkoxysilane, it was infiltrated five times with MeOMgOCO₂Me solution (solid content 0.9 mass%) before adding the TEOS solution and subsequent calcination at 1350°C for 5 h. This process led to a mixture of forsterite (Mg₂SiO₄) as the dominant product, and residual amounts of clinoenstatite, as confirmed by XRD (Fig. 3c) and ²⁹Si MAS nuclear magnetic resonance (NMR) spectroscopy (Fig. 5). In these spectra, the signal at –61.79 ppm can be attributed to Si in Q⁰ coordination mode. This chemical shift has been reported before

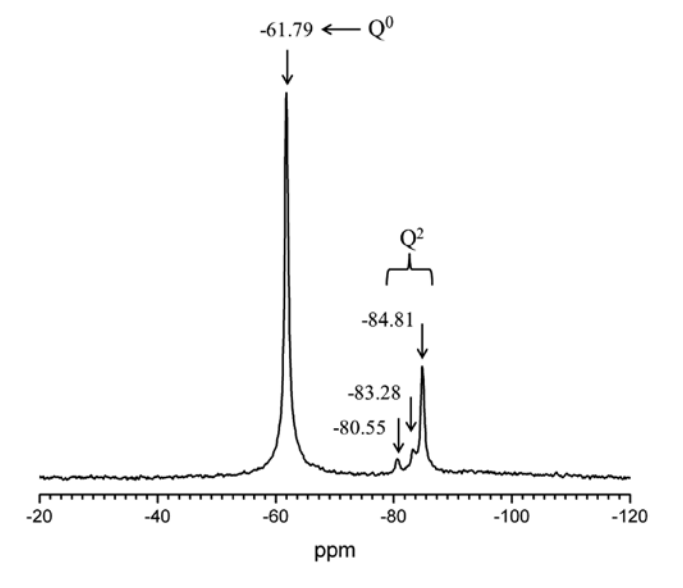


Fig. 5: ²⁹Si MAS NMR spectrum of the sample obtained after five infiltrations with 0.9 mass% MeOMgOCO₂Me solution, subsequent immersion in TEOS solution and calcination at 1350°C for 5 h.

for forsterite [32–34]. Furthermore, three resonances are present at -80.55, -83.28, and -84.81 ppm which can be assigned to ortho or clinoenstatite [32]. Integration of the peak areas indicates a ratio of 78% for Qo (forsterite) and 22% for Q² (ortho or clinoenstatite). These results suggest that when the amount of magnesium is sufficient and the calcination temperature is high enough, then forsterite is formed through a reaction between MgO and the hydrolysed alkoxysilane, as presented in eqs. 4 and 5.

 $MgO + SiO_3$ (amorphous) $\rightarrow MgSiO_3$ (enstatite, metastable)

(4)

$$MgO + MgSiO_3 \rightarrow Mg_2SiO_4$$
 (forsterite) (5)

The replica consists of annealed particles in the range of 500 nm to a few micrometers (Fig. 2d, e). However, shrinkage of the porous monolith was still at $\Delta_{xx} = 31\%$, $\Delta_{rad} = 50\%$ and $\Delta_{tan} = 48\%$. This sample showed a compressive strength of 31 ± 8 MPa (Fig. 4b). The stress-strain curves show the same progression, atypical for ceramic materials, as already observed for the samples calcined at 500°C (Fig. 4a). This confirms that the progression of the curve is due to the samples' micro-, and not their crystal

Samples calcined at 1350°C and containing high Mg contents were obtained by infiltrating MeOMgOCO Me at a solid content of 4.9 mass%, instead of 0.9 mass%, followed by a TEOS treatment. The replica obtained from this process contained a mixture of forsterite and periclase, as shown in the XRD pattern (Fig. 3d). Apparently, under those conditions the initial MgO framework had partly reacted with the silicon precursor resulting in a layer of magnesium silicate. Apparently, only the surface of the magnesium oxide framework which had contact with the silicon precursor had reacted, thus leaving the inner MgO framework intact and yielding a mixture of forsterite and MgO as was evidenced in the XRD pattern. This sample exhibited a compressive strength of 17 ± 3 MPa (Fig. 4c) and reproduced the wood structure such as pit holes precisely. It contained annealed particles in the range of 500 nm to a few micrometers, but exhibited decreased porosity as seen in the SEM image (Fig. 2f). Again, shrinkage was substantial, with $\Delta_{av} = 43\%$, $\Delta_{rad} = 49\%$ and $\Delta_{tan} = 49\%$.

Furthermore, it was attempted to achieve phase-pure forsterite by varying the solid content of the MeOMgO-CO₃Me precursor from 1.5 to 3.1 mass%. However, the replicas obtained from this series only contained mixtures of SiO₂, MgSiO₂ and Mg₂SiO₄ when the solid content of methoxymagnesium methyl carbonate was between 1.5 and 2.2 mass%, and mixtures of MgSiO₃, Mg₂SiO₄ and MgO for the higher solid contents.

2.8 Compressive strength in comparison

The Mg₂SiO₄/MgSiO₅ replica obtained from five times infiltration with MeOMgOCO, Me (solid content 0.9 mass%), subsequent immersion in TEOS solution and calcination at 1350°C for 5 h (see Section 2.7) exhibited a compressive strength (31±8 MPa) which was three times higher than that of a silica replica prepared according to the literature [11] (Fig. 4d).

2.9 BET surface area of forsterite replica

Using nitrogen sorption and evaluation via the BET method, a specific surface area of 0.4 m² · g⁻¹ was determined for the Mg₂SiO₄/MgSiO₃ replica obtained from five infiltrations with MeOMgOCO.Me (solid content 0.9 mass%), subsequent immersion in TEOS solution and calcination at 1350°C for 5 h (see Section 2.7). This replica was selected because it presented the highest compressive strength. It is expected that the thermal conductivity of this material would be larger than that of aerogels, since its specific surface area is significantly lower. Its average pore size is therefore higher than those reported for aerogels, whose specific surface areas lie between 45 and 200 $\text{m}^2 \cdot \text{g}^{-1}$ [16, 17, 35]. Nevertheless, the result suggests that the replicas produced here possess sufficient porosity to be useful as carriers for drugs or sensors, and to a minor extent as insulating material in construction applications.

3 Conclusion

Our study has demonstrated that Mg(OCOOCH₂)(OCH₂) presents a suitable precursor which can penetrate wood cell walls and spread through the cell walls as confirmed by EDS mapping. The macroscopic and submicron scale structures of the wood template are replicated. When more infiltration steps are applied, then a higher amount of magnesium is found in the cell walls and less shrinkage of the replicas occurs. All MgO replicas exhibit poor mechanical stability.

Figure 6 presents the different magnesium-based porous replicas obtained and their properties with respect to the quality of replication and mechanical stability as a function of the specific treatment conditions.

The mechanical stability of the replicas can be improved by subsequent treatment with TEOS solution which results in the formation of a coating comprised of

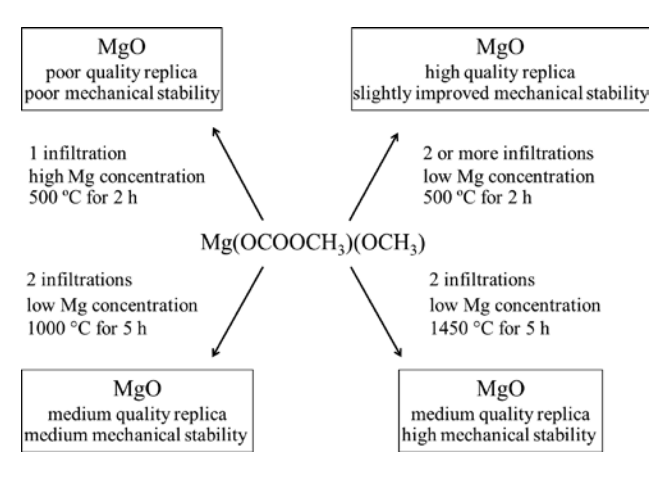


Fig. 6: Overview of different MgO replicas of wood achieved under various treatment conditions with methoxymagnesium methyl carbonate precursor solution.

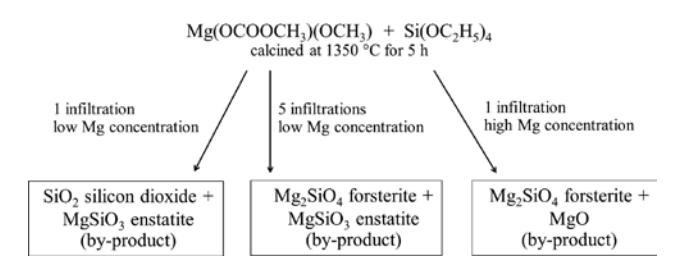


Fig. 7: Summary of the mechanically more stable replicas containing different magnesium silicates.

magnesium silicates (forsterite or enstatite). Depending on the amount of magnesium precursor and TEOS solution applied, different mixtures of magnesium silicates, SiO₂ or MgO are obtained, as presented in Fig. 7. All these products show high compressive strength.

In further experiments, deposition of calcium silicate hydrates, so-called C-S-H (the main constituent of hydrated Portland cement) on the MgO framework should be studied with the aim to achieve exceptional mechanical stability of the replicas.

4 Experimental section

4.1 Preparation of the template

Sections (either cubes with side lengths of 1 cm or radial thin discs of 1 cm (tangential and radial) in diameter and 0.3 mm (axial) in thickness) were cut from the sapwood of pine trees (Pinus sylvestris), weighed and subjected to a series of chemical treatments. In a first step, 150 g of wood was washed by extraction first for 6 h each in a Soxhlet apparatus using 500 mL of a 2:1 by weight mixture of toluene and ethanol and then the same amount of pure ethanol. All samples were stored in ethanol between the processing steps to prevent drying. For preparation of the templates, 1 g of this wood was placed in an oxidizing solution containing 1.4 g of sodium chlorite (NaClO₂) and 0.5 g of acetic acid in 23.1 g of deionized water. Delignification was carried out twice at 70°C for 3 h each whereby the delignification solution was renewed after the initial 3 h. Afterwards, a mild vacuum from a wateriet pump was applied for half an hour. Following the delignification treatment, the templates were immediately extracted with ethanol to remove any residual solutions of reagents [9].

4.2 Infiltration

Magnesium metal in the amount of 2.5 g (0.1029 mol) for high solid content, or 0.5 g (0.0206 mol) for low solid content, was dissolved in 250 mL absolute methanol (dried and stored over molecular sieve, 3 nm) and heated to 65°C to produce a clear solution of Mg(OCH₂)₂. After 90 min of stirring at room temperature, carbon dioxide gas was bubbled through the Mg(OCH₂)₂ solution. A turbid solution of MeOMgOCO, Me had formed which was then centrifuged. The clear solution (~13 g of either 4.9 or 0.9 mass% solid content) was rinsed into a vial containing the pine wood template. Infiltration of the wood cells occurred during the drying process at 70°C. The infiltrated wood template was then kept in an oven at 80°C for 7 h.

4.3 Calcination

To achieve MgO replicas, calcination was performed at various conditions, namely at 500°C for 2 h and at 1450°C for 5 h at a heating rate of 1 K · min-1 with holding steps of 0.5 h each at 200, 330 and 470°C. Immediately after infiltration, hydrolysis of MeOMgOCO₂Me with residual moisture from the wood template occurred and an MgCO₃ sol formed.

The magnesium silicate replicas were synthesized using the magnesium infiltrated templates which were further soaked once with a TEOS solution (1 g TEOS in 8 g EtOH). The infiltrated wood template was then kept in an oven at 80°C for 7 h and subsequently calcined at 1350°C for 5 h at a heating rate of 1 K · min⁻¹. Additional calcination experiments were performed at 200, 330 and 470°C for 0.5 h each and at 600°C for 3 h.

4.4 Analysis

The methoxymagnesium methylcarbonate precursor solution was assessed via dynamic light scattering (DLS) using a Zetasizer Nano ZS apparatus (Malvern Instruments, Workestershire, UK). SEM images of the products obtained from calcination were captured using an XL30 ESEM FEG instrument (Philips/FEI Company, Eindhoven, The Netherlands) equipped with an energy-dispersive X-ray detector (EDX) for elemental analysis (New XL30, EDAX Inc., Mahwah, NJ, USA). The magnesium oxide contained in the replica was identified via X-ray diffraction (D8 advance instrument, Bruker AXS, Bruker, Karlsruhe, Germany). The specific surface area (BET method, N₂) was measured on a Nova 4000e instrument from Quantachrome (Boynton Beach, FL, USA) utilizing a sample degassed for 2 h at 200°C. Additionally, the forsterite polymorph contained in the replicas was identified by ²⁹Si solid state MAS NMR spectroscopy (Bruker).

Mechanical testing was carried out in plate-plate compression geometry adapted from DIN/EN/ISO-844 on a smarTens010 universal testing machine (Karg Industrietechnik, Krailing, Germany). The plate size was reduced to 4 cm² to account for our small sample sizes. Each measurement was repeated three times and the values reported for the compressive strength samples represent the average.

Acknowledgment: The authors gratefully acknowledge financial support by the German Research Foundation (Deutsche Forschungsgemeinschaft, DFG) within the framework of the priority program SPP 1420.

References

- [1] K. Raed, U. Gross, Int. J. Thermophys. 2009, 30, 1343.
- [2] S. S. Kistler, Nature 1931, 127, 741.
- [3] S. S. Kistler, J. Phys. Chem. 1932, 36, 52.
- [4] Z. Wang, Z. Pan, Appl. Surf. Sci. 2015, 356, 1168.
- [5] A. D. C. Permana, A. Nugroho, K. Y. Chung, W. Chang, J. Kim, Chem. Eng. J. 2014, 241, 216.
- [6] P. Fratzl, R. Weinkamer, Pro. Mater. Sci. 2007, 52, 1263.
- [7] D. Fengel, G. Wegener, A. Greune, Wood Sci. Technol. 1989, 23, 123.

- [8] H. F. Jacob, D. Fengel, S. E. Tschegg, P. Fratzl, Macromolecules 1995, 28, 8782.
- [9] P. A. Ahlgren, W. Q. Yean, D. A. I. Goring, Tappi J. 1971, 54, 737.
- [10] L. Sapei, R. Nöske, P. Strauch, O. Paris, Chem. Mater. 2008, 20, 2020.
- [11] D. Van Opdenbosch, G. Fritz-Popovski, O. Paris, C. Zollfrank, J. Mater. Res. 2011, 26, 1193.
- [12] G. Fritz-Popovski, D. Van Opdenbosch, C. Zollfrank, B. Aichmayer, O. Paris, Adv. Funct. Mater. 2013, 23, 1265.
- [13] D. Van Opdenbosch, M. H. Kostova, S. Gruber, S. Krolikowski, P. Greil, C. Zollfrank, Wood Sci. Technol. 2010, 44, 547.
- [14] M. H. Kostova, M. Batentschuk, F. Goetz-Neunhoeffer, S. Gruber, A. Winnacker, P. Greil P, C. Zollfrank, Mater. Chem. Phys. 2010, 123, 166.
- [15] M. H. Kostova, C. Zollfrank, M. Batentschuk, F. Goetz-Neunhoeffer, A. Winnacker, P. Greil, Adv. Funct. Mater. 2009, 19,599.
- [16] T. Kornprobst, J. Plank, GDCh-Monographie: Tagung Bauchemie 2010, 42, 121.
- [17] J. Plank, H. Hoffmann, J. Schölkopf, W. Seidl, I. Zeitler, Z. Zhang, Res. Lett. Mater. Sci. 2009, 2009, 1.
- [18] T. Kornprobst, J. Plank, J. Non-Cryst. Solids 2013, 361, 100.
- [19] A. Kosak, A. Lobnik, Int. J. Appl. Ceram. Technol. 2015, 12, 461.
- [20] J. Ita, L. Stixrude, J. Geophys. Res. 1992, 97, 6849.
- [21] S. Ramesh, A. Yaghoubi, K. Y. Sara Lee, K. M. Christopher Chin, J. Purbolaksono, M. Hamdi, M. A. Hassan, J. Mech. Behav. Biomed. Mater. 2013, 25, 63.
- [22] S. Ni, L. Chou, J. Chang, Ceram. Int. 2007, 33, 83.
- [23] M. Kharaziha, M. H. Fathi, Ceram. Int. 2009, 35, 2449.
- [24] M. Kharaziha, M. H. Fathi, J. Mech. Behav. Biomed. Mater. **2010**, 3, 530.
- [25] C. Y. Tan, R. Singh, Y. C. Teh, Y. M. Tan, Int. J. Appl. Ceram. Technol. 2015, 12, 437.
- [26] S. Klaithong, D. Van Opdenbosch, C. Zollfrank, J. Plank, Z. Naturforsch. 2013, 68b, 533.
- [27] V. Merk, M. Chanana, T. Keplinger, S. Gaan, I. Burgert, Green Chem. 2015, 17, 1423.
- [28] H. D. Lutz, Z. Anorg. Allg. Chem. 1967, 353, 207.
- [29] H. Thoms, M. Epple, H. Viebrock, A. Reller, J. Mater. Chem. 1995, 5, 589,
- [30] H. L. Finkbeiner, M. Stiles, J. Am. Chem. Soc. 1963, 85, 616.
- [31] K. X. Song, X. M. Chen, X. C. Fan, J. Am. Ceram. Soc. 2007, 90, 1808.
- [32] J. F. Stebbins, W. R. Panero, J. R. Smyth, D. J. Frost, Am. Mineral. 2009, 94, 626.
- [33] J. F. Stebbins in Mineral Physics and Crystallography: A Handbook of Physical Constants, Vol. 2 (Ed.: T. J. Ahrens), American Geophysical Union, Washington, DC, 1995, p. 303.
- [34] J. M. Griffin, S. E. Ashbrook, Annu. Rep. NMR Spectrosc. 2013, 79, 241.
- [35] H. Zheng, C. Gao, S. Che, Micropor. Mesopor. Mater. 2008, 116, 299.